NANO LETTERS

2002
Vol. 2, No. 4
279−283

Near-Field Imaging of Nonlinear Optical Mixing in Single Zinc Oxide Nanowires

Justin C. Johnson, Haoquan Yan, Richard D. Schaller, Poul B. Petersen, Peidong Yang, and Richard J. Saykally*

Department of Chemistry, University of California, Berkeley, California 94720-1460

Received November 30, 2001; Revised Manuscript Received January 16, 2002

ABSTRACT

The nonlinear optical response of semiconductor nanowires has potential application for frequency conversion in nanoscale optical circuitry. Here, second- and third-harmonic generation (SHG, THG) are imaged on single zinc oxide (ZnO) nanowires using near-field scanning optical microscopy (NSOM). The absolute magnitudes of the two independent $\chi^{(2)}$ elements of a single wire are determined, and the nanowire SHG and THG emission patterns as a function of incident polarization are attributed to the hexagonal nanowire geometry and $\chi^{(2)}$ tensor symmetry.

Semiconductor nanowires are of current interest because of their unique electrical and optical properties.[1−3] In particular, their nonlinear optical properties suggest potential applications as frequency converters or logic/routing elements in nanoscale optoelectronic circuitry. A linear optical property of nanowires, photoluminescence (PL) polarization, has recently been studied in single indium phosphide nanowires.[2] In that case, the PL polarization is based upon the classical electromagnetic properties of a dielectric cylinder and averages ca. 91%. In contrast, coherent nonlinear optical phenomena, such as second- and third-harmonic generation (SHG and THG, respectively), depend explicitly on the crystal lattice structure of the medium, which could yield a very high (nearly 100%) polarization selectivity. In addition, the temporal response of the nonresonant harmonic generation is similar to the pulse width of the pump laser, in some cases ≈20 fs,[4] while incoherent processes are at least 2−4 orders of magnitude slower. Moreover, nonresonant SHG is essentially independent of wavelength below the energy band gap of semiconductor materials, most often including the 1.3−1.5 μm wavelength region typically used in optical fiber communications. Hence, characterizing the nonlinear response of individual nanowires is crucial for evaluating potential applications of the nanowires as active building blocks for large bandwidth photonic applications; however, there have been no previous studies of the nonlinear optical properties of single semiconductor nanowires.

A material of particular interest is zinc oxide (ZnO), a wide band gap (3.37 eV, 368 nm) semiconductor that has been the subject of many recent studies because of its potential as a UV-blue emitter for lasers and diodes.[5,6] Huang et al. have recently reported lasing behavior in ZnO nanowires,[3] and the properties of individual ZnO nanolasers have been studied with near-field scanning optical microscopy (NSOM).[7] In addition, studies of microcrystalline ZnO thin films[4,8] have revealed a large second-order nonlinearity, characterized by $\chi^{(2)}$, which determines the efficiency of a material as a converter of optical frequencies via several processes (e.g., second-harmonic generation (SHG) and sum- and difference- frequency generation (SFG, DFG)). In this report, NSOM is used to image SHG and THG from single ZnO nanowires, which demonstrate a large, highly polarization-dependent nonlinear response.

The vertical ZnO nanowires (Figure 1a) were removed from the growth substrate by sonication and dispersed onto a flat sapphire substrate for NSOM studies,[9,10] which produce simultaneous topographic and optical images with high spatial resolution (<100 nm). NSOM has previously been utilized in several experiments involving second-order nonlinear processes,[11−14] mainly to study boundaries or interfaces in centrosymmetric materials, which are dipole-forbidden to have a second-order response except at surfaces, where the symmetry is broken.[15] We employ the oblique collection mode NSOM, in which the sample is illuminated in the far-field, as is preferred for nonlinear near-field imaging because of the requirement for high incident pulse intensities.[16] Figure 1b depicts the experimental laser beam geometry with respect to an arbitrarily oriented nanowire on the sapphire substrate. The hexagonal crystal structure gives the nanowires six prismatic side faces, each of which is oriented at a distinct angle to the incident beam. The face labeled "front" is nearly normal to the incident beam (for $\phi \approx 0$). This particular laser beam/nanowire geometry produces a pattern of three parallel areas of signal along the wire. Figure 2 shows SHG images of single nanowires with a $\phi \approx 0$ geometry. The incident laser is p-polarized for Figure

* To whom correspondence should be addressed. E-mail: saykally@uclink.berkeley.edu.

10.1021/nl015686n CCC: $22.00
Published on Web 02/19/2002

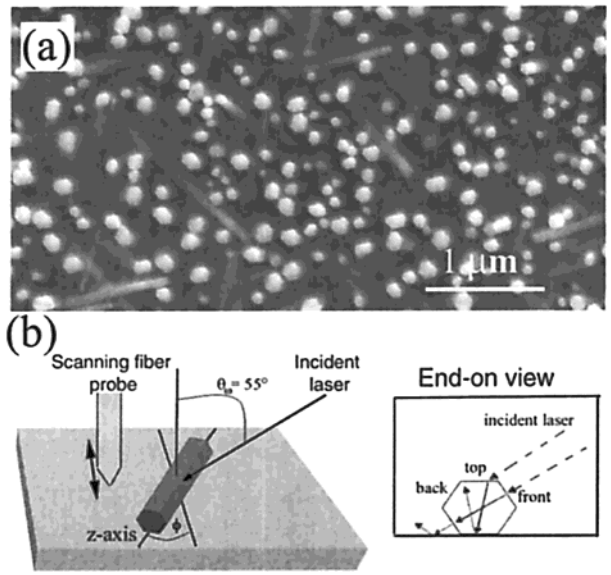

Figure 1. Zinc oxide nanowire array and SHG NSOM experimental configuration. (a) Scanning electron micrograph of ZnO nanowire array (end-on view) showing hexagonal end faces. The wires are nucleated with gold and grow vertically from the sapphire (110) plane.[25] (b) Illustration of the sample/beam geometry. The surface normal and the fundamental beam **k**-vector form the angle θ, which was fixed during the experiment. The angle ϕ is formed between the nanowire symmetric axis and the normal to the propagation vector of the incident beam in the sample plane. The polarization angle, α, is varied during the experiment. The inset shows a cross-sectional view of the fundamental (dashed) and SHG (solid) beam geometry. Two primary SHG paths are shown: one transmitted through the top face, and the other through the side face. The transmitted angle (measured from the surface normal) through the top face is approximately 24°.

2a and s-polarized for Figure 2b. The spatial resolution in the optical images is approximately 100 nm. The signal traces below each image show the signal levels across the corresponding wire. The overall signal level in Figure 2b is about 9 times larger than that in Figure 2a, which is due to the probing of different $\chi^{(2)}$ components with different polarizations, as discussed in detail below. The SHG collected in Figure 2 originates from both the bulk and the surface of the nanowire, since ZnO has a noncentrosymmetric hexagonal (6 mm) crystal structure. However, SHG in bulk ZnO cannot be phase matched;[17] therefore the most efficient generation of SHG occurs in a surface layer approximated by the coherence length, which for ZnO is still larger than the nanowire diameter (>1 μm compared to 50−100 nm).

The total detected SHG signal is a function of $\chi^{(2)}$ and other optical parameters of the material:[8]

$$I_{2\omega} \propto {I_\omega}^2 {T_\omega}^2 |\chi^{(2)}_{\text{eff}}|^2 \frac{\sin^2 \Phi}{\Phi^2} \quad (1)$$

Here, $\chi_{\text{eff}}^{(2)}$ is the effective second-order susceptibility for an arbitrary input and output polarization, T_ω is the Fresnel factor for transmission of the incident beam, I_ω is the beam intensity, and Φ is the phase mismatch of the fundamental and second-harmonic beams.[18] From consideration of Fresnel factors and the effective intensity of the laser (number of photons per unit area) incident at each face, the ratio of SHG signal levels front/top (determined from the line traces) for p-polarized excitation is expected to be about 1.5. For s-polarized incident light, the ratio is approximately 4.2. The data from Figure 2a for p-polarization give a ratio of 1.6, while the s-polarized trace in Figure 2b gives a ratio of approximately 5.0. Both traces give a front/back ratio of about 1.4, which is probably due to loss of collected signal on the opposite side face due to multiple reflections (nanowire−air and air−substrate, Figure 1b inset). The close agreement between the calculated and measured values confirms that the altered incident intensity from Fresnel factors and nanowire geometry are responsible for the patterns found in the $\phi \approx 0$ images. Wires with a significantly larger ϕ value (>30°) showed a more homogeneous SHG signal (primarily from the top face, Figure 3d) because of the different input coupling caused by an increase in the incident angles on the side faces.

Figure 3 shows two series of SHG images, illustrating the input polarization and nanowire orientation dependence of the SHG. This dependence arises from the two independent, nonvanishing components of $\chi^{(2)}$ observed in SHG for ZnO, $\chi^{(2)}_{zxx}$ and $\chi^{(2)}_{zzz}$.[8,19] By using the $\chi^{(2)}_{\text{eff}}$ values from the transformed coordinates, one is able to derive the ratio of the two components, $\chi^{(2)}_{zxx}$ and $\chi^{(2)}_{zzz}$. $\chi^{(2)}_{\text{eff}}$ for an arbitrary linear polarization is given by

$$\chi^{(2)}_{\text{eff}} = \{(\cos^2\theta_{2\omega} + \cos^2\phi \sin^2\theta_{2\omega})[(\cos\alpha\cos\phi + \sin\alpha\sin\phi\cos\theta_\omega)^4(\chi^{(2)}_{zzz})^2 + ((\cos\alpha\sin\phi + \sin\alpha\cos\phi\cos\theta_\omega)^4 + (\sin\alpha\sin\theta_\omega)^4)(\chi^{(2)}_{zxx})^2]\}^{1/2} \quad (2)$$

ϕ and θ are the angles defined in Figure 2a, and α is the polarization angle (s = 0, p = π/2). In Figure 3a,b the wires are situated approximately normal to each other, with an s-polarized incident beam in Figure 3a and p-polarization in Figure 3b. The polarization ratio ($SHG_{s-inc}/(SHG_{p-inc} + SHG_{s-inc})$) for wire 1 is 0.90. Wire 2 (oriented at $\phi \approx 0$) has an average signal that is 2.5 times that of wire 1 (oriented at $\phi \approx 90°$). $\chi^{(2)}_{\text{eff}}$ and eq 1 predict that the maximum signal level for a wire with $\phi \approx 90°$ should be smaller than that of a wire with $\phi \approx 0°$ by $(\cos\theta)^{-6} = 1.72$, if the wires are the same size. For wires of different diameters, one must consider that $\chi^{(2)}$ is a material response that depends on the number of molecules probed (N) and the average hyperpolarizability $\langle\beta\rangle$ of the ZnO lattice in the sample region in which SHG occurs (neglecting local fields),[20]

$$\chi^{(2)} \approx N\langle\beta\rangle \quad (3)$$

where the value of β for a single crystal nanowire should be spatially invariant, except for surface effects. In Figure 3a, wire 2 has a diameter that is 20% larger than wire 1; thus the signal from wire 2 should be additionally 44% larger. Considering these factors, the signal ratios agree well with theoretical predictions.

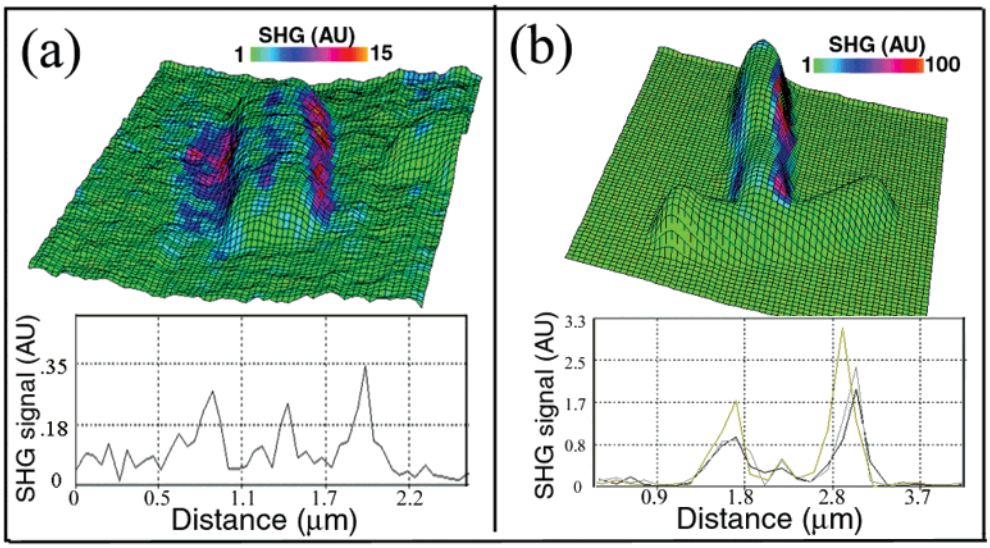

Figure 2. Near-field SHG images of single ZnO nanowires. (a) Combined topographical and SHG image of a ZnO wire with $\phi \approx 0°$. $\omega = 800$ nm, p-polarized beam is incident from the right. Overall image size is $(6\ \mu m)^2$, maximum topographic height is 70 nm. Below: SHG signal trace across the wire. (b) SHG image of a single ZnO wire ($\phi \approx 0°$). Maximum topographic height is 100 nm, image size is $(10\ \mu m)^2$. Below: signal traces taken across the upper wire. There was significant variation in SHG signal along the length of the wire, so the three traces were taken at the two ends and the center, and the average is considered in the calculations. The hexagonal structure of the nanowires and the use of a large taper angle near-field probe can result in topographical images that do not correctly reproduce the nanowire dimensions (the images are a convolution of tip and sample features). The measurement of the height of the sample remains accurate, but the lateral features can be broadened due to the widening of the probe along the etched cone angle. Also, the SHG signal patterns are inconsistent with suggested NSOM artifacts, considering that the fundamental wavelength is not detected and the incident polarization is parallel to the front face of the nanowire.[26]

Parts d−e of Figure 3 show nanowires at various orientations to the incident laser beam. The polarization in Figure 3d is along the axis of the wire 1, while the polarization in Figure 3e is rotated by 90°. The polarization ratio for wire 1 ($\phi \approx 125°$) is about 0.95. With particular geometries, the polarization ratio for the wires can reach nearly 1.0, although no systematic effort was made to achieve this maximum polarization ratio. The maximum SHG signal for each wire occurs when the polarization is along the nanowire symmetry axis, in which case $\chi^{(2)}_{zzz}$ is probed. Theoretical predictions for a 6 mm lattice suggest that SHG cannot be efficiently generated with the incident beam propagation direction exactly parallel to the symmetry axis of the nanowire because the polarization of the SHG must also be along this same direction.[19] This is consistent with our experimental results, in which case the largest SHG signal was collected near the side faces of nanowires situated normal to the incident laser. In contrast, efficient THG can be realized by pumping the nanowire along the symmetry axis, as demonstrated in Figure 4a, in which nanowires with $\phi \approx 90°$ exhibit large THG signal along the wire. Several $\chi^{(3)}$ components can contribute to the third-order response in this case,[21] thus allowing the bulk-generated THG signal to be relatively strong. As predicted, the same wires exhibited very little SHG contrast (Figure 4b). The power dependence of each process (Figure 4, inset) demonstrates the threshold nature of the SHG and THG emission.

To quantitatively analyze the SHG polarization effect, polarization traces were taken on several wires from Figure 3. The near-field probe was maintained above each wire, and the input polarization was rotated as the SHG signal was monitored (Figure 3c,f). The theoretical traces were computed using eq 1, $|\chi^{(2)}_{eff}|^2$, the measured angles ϕ and θ, and the derived ratio of $\chi^{(2)}_{zxx}$ and $\chi^{(2)}_{zzz}$. The polarization data were fit to theory (eq 2) and nearly all the wires tested (diameters 80−100 nm) exhibited a ratio $\chi^{(2)}_{zzz}/\chi^{(2)}_{zxx}$ of approximately 2.0−2.3, while one larger wire (diameter 120−130 nm) exhibited $\chi^{(2)}_{zzz}/\chi^{(2)}_{zxx} = 4.2$. These ratios can be compared with a value of 3.0 for bulk crystalline ZnO[22] to as high as 6.0 for polycrystalline thin films.[8] $\chi^{(2)}_{zxx}$ represents the second-order lattice response perpendicular to the symmetric axis, which is the direction most confined by the quasi-1D nature of the nanowire. Thus, one might expect the enhancement of $\chi^{(2)}_{zxx}$ to be larger than that of $\chi^{(2)}_{zzz}$, given that $\chi^{(2)}_{eff} = \chi^{(2)}_{bulk} + \chi^{(2)}_{surface}$, where $\chi^{(2)}_{surface}$ can be enhanced relative to $\chi^{(2)}_{bulk}$[23] and that surface effects have a larger contribution to $\chi^{(2)}_{zxx}$ than to $\chi^{(2)}_{zzz}$. Enhancement of $\chi^{(2)}$ has been studied for spherically symmetric quantum materials,[20] but no previous study of the enhancement of individual components of the $\chi^{(2)}$ tensor has been performed. SHG measurements on microcrystalline thin films appear to produce the opposite effect: $\chi^{(2)}_{zzz}$ is enhanced due to the constraint of the film thickness (<100 nm) rather than the diameter of the crystal.[7] A recent redetermination of the $\chi^{(2)}$ components for bulk crystalline ZnO[24] suggests that the ratio $\chi^{(2)}_{zzz}/\chi^{(2)}_{zxx}$ is as high as 10, which further indicates an enhancement of $\chi^{(2)}_{zxx}$ from our single wire measurements compared to bulk.

Using a reference material, one can determine the absolute magnitude of each component of $\chi^{(2)}$ for individual nanowires. $\chi^{(2)}_{zxx}$ and $\chi^{(2)}_{zzz}$ were determined by measuring the nanow-

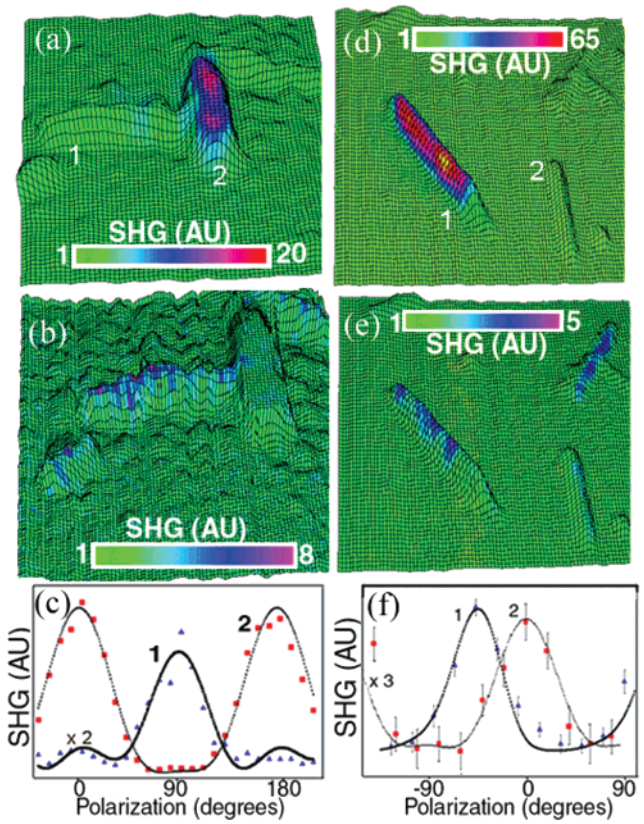

Figure 3. Nanowire SHG polarization dependence. (a) Combined topographical and SHG image of two wires at an angle of approximately 90°. The image size is (13 μm)^2 and the maximum topographic height is 130 nm. The beam is s-polarized, incident from the right. (b) SHG of same region as in (a) with the p-polarized incident beam. (c) Polarization-dependent SHG data and theoretical predictions taken from the wires labeled in (a). The theoretical curves are calculated from eq 2 for the SHG signal and $\chi^{(2)}_{\text{eff}}$ for a hexagonal crystal. (d) Image of (16 μm)^2 region showing several nanowires. Maximum topographic height is 120 nm. The polarization $\alpha = -45°$. (e) Image of the same region as in (d) with polarization $\alpha = 45°$. (f) Polarization traces taken from the wires labeled 1 and 2 in (c) and theoretical simulations.

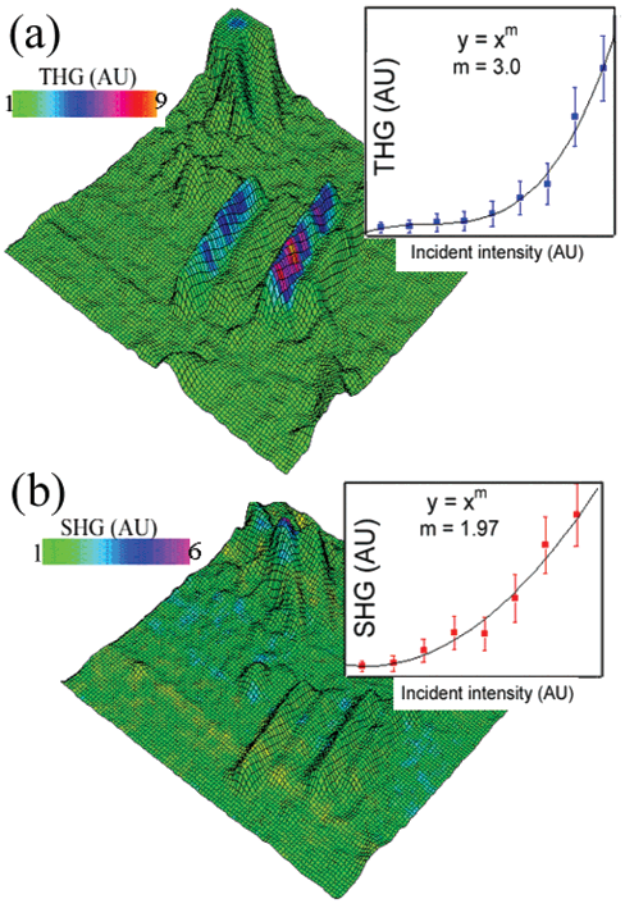

Figure 4. Third- and second-harmonic NSOM images of single ZnO nanowires. (a) THG image of several nanowires, the two center wires being oriented at $\phi \approx 90°$. The laser beam is incident from the lower left in the figure. Total image size is (12 μm)^2, and maximum topographic height is 90 nm. Inset: incident beam power dependence of the THG and third-order fit. (b) SHG image of the same region as in (a), with the wires at $\phi \approx 90°$ showing minimal contrast. Inset: input power dependence of the SHG signal with second-order fit. The order of the polynomial was determined by performing a least squares linear fit to the data on a logarithmic scale. For the THG and SHG images, $\lambda_{\text{inc}} = 1320$ and 800 nm, respectively.

ire SHG with respect to a zinc selenide (ZnSe) disk (at 1.4 μm excitation). Careful measures were taken to maintain the pump beam and collection conditions for the reference measurements, but it should be noted that the values of $\chi^{(2)}_{zxx}$ and $\chi^{(2)}_{zzz}$ can only be determined approximately. The coherence lengths of ZnO and ZnSe are not necessarily equivalent but both should be considerably larger than the depth of field of the near-field microscope ($\ll\lambda$). Efforts were made to sample the SHG signal at many points on the nanowire to obtain the average signal level, independent of local waveguiding[7] or scattering effects. A disk of zinc sulfide was also referenced to test the consistency of the method, and its $\chi^{(2)}_{\text{eff}}$ was found to be 17 pm/V, in relatively good agreement with literature values (14 pm/V).[22] Using the ZnSe reference (78 pm/V), $\chi^{(2)}_{zzz}$ for a single ZnO wire (not shown) = 5.5 pm/V and $\chi^{(2)}_{zxx} = 2.5$ pm/V. The $\chi^{(2)}_{zzz}$ value is considerably lower than the reported bulk value (18 pm/V) but in relatively good agreement with values reported for ZnO thin films (4−10 pm/V). One of the possible reasons for the lower value compared to bulk ZnO is that the number of ZnO molecules probed for a single nanowire is less than those probed on a solid disk. If one considers the fiber probe collection region to be roughly a cylinder (with a diameter equal to the optical aperture and a length equal to the depth of field) below the probe, then the nanowire will not necessarily fill this cylinder whereas a solid disk does. Estimates of the loss of signal from insufficient filling make the nanowire $\chi^{(2)}_{zzz}$ value greater by 1.5−3 times, resulting in better agreement with the aforementioned far-field experiments.

In summary, we have shown that single ZnO nanowires exhibit a high nonresonant second-order nonlinearity that follows a theoretical model based upon a hexagonal lattice structure. Variations of the SHG and THG signal as a function of position on single wires follow simple geometrical and optical considerations. A large polarization dependence, dictated by the asymmetry of the nonlinear susceptibility, is exhibited in the SHG images. The nanowire

SHG was found to be primarily wavelength independent ($\lambda_{SHG} > 400$ nm) and relatively efficient, with a larger $\chi^{(2)}_{eff} \geq 5.5$ pm/V than β-barium borate (BBO, $\chi^{(2)}_{eff} \approx 2.0$ pm/V), a commonly used doubling crystal. The nonlinear optical properties demonstrated here suggest that ZnO nanowires could be effectively employed as frequency converters or logic components in nanoscale optoelectronics.

Acknowledgment. P.Y. and H.Y. are supported in part by a New Faculty Award from Dreyfus Foundation, a Career Award from the National Science Foundation, Research Corp., Department of Energy, and start-up funds from the University of California, Berkeley. P.Y. is an Alfred P. Sloan Research Fellow. P.Y. thanks the 3M Co. for an untenured faculty award. R.J.S., R.D.S, P.B.P., and J.C.J are supported by the Physical Sciences Division of the National Science Foundation.

References

(1) Yu, J.; Chung, S.; Heath, J. R. *J. Phys. Chem. B* **2000**, *104*, 11864.
(2) Wang, J.; Gudiksen, M. S.; Duan, X.; Cui, Y.; Lieber, C. M. *Science* **2001**, *293*, 1455.
(3) Huang, M. H.; Mao, S.; Feick, H.; Yan, H.; Wu, Y.; Kind, H.; Weber, E.; Russo, R.; Yang, P. *Science* **2001**, *292*, 1897.
(4) Griebner, U.; Kaindl, R. A.; Elsaesser, T.; Seeber, W. *Appl. Phys. B* **1998**, *67* 757.
(5) Fejer, M. J. *Phys. Today* **1994**, *47*, 25.
(6) Bagnall, D. M.; Chen, Y. F.; Zhu, Z.; Yao, T.; Shen, M. Y.; Goto, T. *Appl. Phys. Lett.* **1998**, *73*, 1038.
(7) Johnson, J. C.; Yan, H.; Schaller, R. D.; Haber, L. H.; Saykally, R. J.; Yang, P. *J. Phys. Chem. B* **2001**, *105*, 11387.
(8) Cao, H.; Wu, J. Y.; Ong, H. C.; Dai, J. Y.; Chang, R. P. H. *Appl. Phys. Lett.* **1998**, *73*, 572.
(9) Schaller, R. D.; Johnson, J. C.; Saykally, R. J. *Anal. Chem.* **2000**, *72*, 5361.
(10) A chemically etched optical fiber was held at a constant distance (<10 nm) from the sample by a shear-force feedback mechanism. The excitation source for 800 nm/400 nm SHG measurements was a regeneratively amplified Ti:sapphire laser (80 fs, 800 nm, 2.0 W, 1 kHz) that was attenuated to <1 mW and focused onto the sample to a spot size of approximately 100 μm in diameter. Near-infrared wavelengths were generated by using the Ti:sapphire amplifier to pump an optical parametric amplifier, which has a tunable signal/idler wavelength of 1.2−2.7 μm. The polarization of the incident light was controlled with a $\lambda/2$ waveplate. The identity of the SHG and THG signal was confirmed by observing the spectrum with a monochromator and CCD and by performing a power-dependence using a stepped-index neutral density filter.
(11) Shen, Y.; Markowicz, P.; Winiarz, J.; Swiatkiewicz, J.; Prasad, P. N. *Opt. Lett.* **2001**, *26*, 725.
(12) Bozhevolnyi, S. I.; Vohnsen, B.; Pedersen, K. *Opt. Commun.* **1998**, *150*, 49.
(13) Schaller, R. D.; Saykally, R. J. *Langmuir* **2001**, *17*, 2055.
(14) Schaller, R. D.; Roth, C.; Raulet, D.; Saykally, R. J. *J. Phys. Chem. B* **2000**, *104*, 5217.
(15) Shen, Y. R. *Principles of Nonlinear Optics*; Wiley: New York, 1984.
(16) Smolyaninov, I. I.; Lee, C. H.; Davis, C. C.; Rudin, S. *J. Microscopy* **1999**, *194*, 532.
(17) Kurtz, S. K.; Perry, T. T. *J. Appl. Phys.* **1968**, *39*, 3798.
(18) The phase mismatch term is neglected in the calculations. As discussed in ref 9, phase-matching is thought to be relaxed in near-field experiments. Moreover, the sample thickness probed is much smaller than the coherence length. Therefore, it is expected that phase-matching effects will be negligible.
(19) The subscript coordinates symbolize the polarization direction of the second-harmonic and the fundamental photons with respect to the crystal axes. The only allowed SHG in this experiment has polarization along the crystal *z*-axis, which is the symmetric axis of the nanowire.
(20) Jacobsohn, M.; Banin, U. *J. Phys. Chem. B* **2000**, *104*, 1.
(21) $\chi^{(3)}$ for a ZnO lattice has components that allow for x and y polarized THG output (e.g., $\chi^{(3)}_{xxxx}$ and $\chi^{(3)}_{yyyy}$). Also, two crossed-polarization fields would probe nonvanishing components of $\chi^{(2)}$ with SFG polarized perpendicularly to the *z*-axis of the nanowire.
(22) Sutherland, R. L. *Handbook of Nonlinear Optics*; Dekker: New York, 1996.
(23) Shen, Y. R. *IEEE J. Sel. Top. Quantum Electron.* **2000**, *6*, 1375.
(24) Wang, G.; Wong, G. K. L.; Ketterson, J. B. *Appl. Opt.* **2001**, *40*, 5436.
(25) Huang, M. H.; Wu, Y.; Feick, H.; Yang, P. *Adv. Mater.* **2001**, *13*, 113.
(26) Hecht, B.; Sick, B.; Wild, U. P.; Deckert, V.; Zenobi, R.; Martin, O. J. F.; Pohl, D. W. *J. Chem. Phys.* **2000**, *112*, 7761.

NL015686N